Published in Materials Research Society Symposium Proceedings Vol. 640 © 2001 Materials Research Society

Reaction Kinetics of Thermally Stable Contact Metallization on 6H-SiC

Robert S. Okojie, Dorothy Lukco[1], Yuan L. Chen[2], David Spry[3] and Carl Salupo[3]
NASA Glenn Research Center, Instrumentation and Controls Division
21000 Brookpark Road, M/S 77-1, Cleveland OH 44135; (216) 433-6522
[1]AYT 20001 Aerospace Parkway, Brookpark, OH 44142.
[2]Dynacs Engineering Company, Inc., 21000 Brookpark Rd. Bldg. 500 Brookpark, OH 44135
[3]Akima Corporation, Fairview Park, OH 44126.

ABSTRACT

The growth kinetics of thermally stable Ti(100nm)/$TaSi_2$ (200nm)/Pt (300nm) metallization on 6H-SiC was studied after heat treatment in air up to 700^{o}C. Scanning electron microscopy (SEM) of the contact surface morphology reveals a two-dimensional network of features that is attributed to non-uniform oxide growth associated with the multigrain structure of the platinum overlayer. Auger electron spectroscopy (AES) and high-resolution transmission electron microscopy (HRTEM) identified three important reaction zones after initial 30-minute anneal at 600^{o}C in nitrogen. One is the formation of a platinum silicide overlayer resulting from $TaSi_2$ decomposition. The second is titanium silicide formation adjacent to the decomposed $TaSi_2$. The third is pseudo-epitaxial Ti_5Si_3 at the SiC interface. Specific contact resistance values ranging from 10^{-4}-10^{-6} Ω-cm^2, remained stable after 200 hours at 600^{o}C in air. Activation energies of 1.03eV for platinum silicide oxidation and 1.96eV for Ti_5Si_3 are obtained from Arrhenius plots.

INTRODUCTION

There is a growing interest in the use of silicon carbide (SiC) as the wide bandgap (WBG) semiconductor of choice for electronics and sensors in high power and harsh environments. However, unresolved reliability issues, prominent among which is stable contact metallization, temper this growing interest in SiC. Thermal stability of electrical contacts is a fundamental requirement for reliable electronics and sensing devices operating in harsh environments. Aggressive packaging methodologies have been adopted that provide hermetic sealing against contact oxidation, but these suffer from the drawbacks of added complexity, cost, and new reliability issues. Also, in the course of testing SiC devices, the need to expand the research effort beyond the traditionally focused investigation of the immediate metal/SiC interface has become evident. The traditional approach will not guarantee long term contact stability because it ignores broader failure mechanisms that exist elsewhere.

The effort at NASA Glenn Research Center (GRC) has adopted a more global strategy by coupling interconnect, fabrication, and packaging principles toward achieving stable electrical contacts on SiC. The result presented here is an attempt to develop a thermochemical model of Ti/$TaSi_2$/Pt metallization on 6H-SiC that will serve as a building block for future SiC device implementation at NASA-GRC. Analytical tools such as SEM, AES, and HRTEM are used to extract reaction parameters that allow for better understanding of the reaction kinetics.

EXPERIMENTAL

6H-SiC, off-axis (3.5^o) and (0001)-oriented, high resistivity p-type substrates with 0.5 μm thick n-type epilayer (N_d-N_a = 2x10^{19}cm^{-3}) were purchased from Cree Research [1]. The wafers were

inspected as received and surface features were mapped using a high-resolution Nomarski optical microscope. The samples were initially cleaned in 50:50 H_2SO_4:H_2O_2 solution for 15 minutes, followed by a De-Ionized (DI)-water rinse. Dry oxidation followed at 1150^{o}C in 2 sccm of ULSI-grade oxygen for three hours. The samples were then dipped in 49%HF to strip the oxide. Dry etching in NF_3 and argon was used to etch mesa strips in the n-type epilayer, thereby creating an n-p junction in a four-point probe configuration. A second 5-hour dry oxidation and oxide via etching was followed by metal deposition and patterned etching. A more detailed description of this process can be found elsewhere [2].

The samples were split into three sets, each containing one patterned and one unpatterned sample. The first set was treated in air at 500^{o}C while the second and third sets were treated in air at 600^{o}C and 700^{o}C, respectively. The sample sets were cooled at various time intervals so that both material analysis and electrical characterization could be performed.

RESULTS AND DISCUSSION

Accurate prediction of the dominant reaction mechanisms in a multilayer metallization system is generally an arduous task. Therefore, we identified surface oxidation of the platinum silicide and titanium silicide formation at the SiC interface zone as the two most critical reaction mechanisms for long-term electrical and mechanical stability of the contact. Other reactions within these zones are assumed to play a less active role since they remained relatively immobile in this experiment. This led to the development of a predictive reaction model for oxidation and silicidation of the metallization on 6H-SiC. The theoretical analysis relied on the growth kinetics developed by Deal *et al* [3] for silicon oxidation and Nathan *et al* [4] for silicide formation. Reaction rates and activation energies were extracted from experimental data and used as first order approximation of the long-term reactions occurring at these critical zones. The cross section HRTEM of the as-deposited sample is shown in Figs. 1(a-c). Figures 1a and c are magnified sections of Fig. 1b that highlight interface zones of Ti/SiC and Pt/$TaSi_2$, respectively. Measured lattice parameters confirmed epitaxial titanium (*a=0.295 nm, c=0.468 nm*) during sputter deposition as shown in Fig. 1a. In Fig. 1b, the platinum layer has columnar structures with a section magnified and shown in Figure 1c to reveal multigrain features.

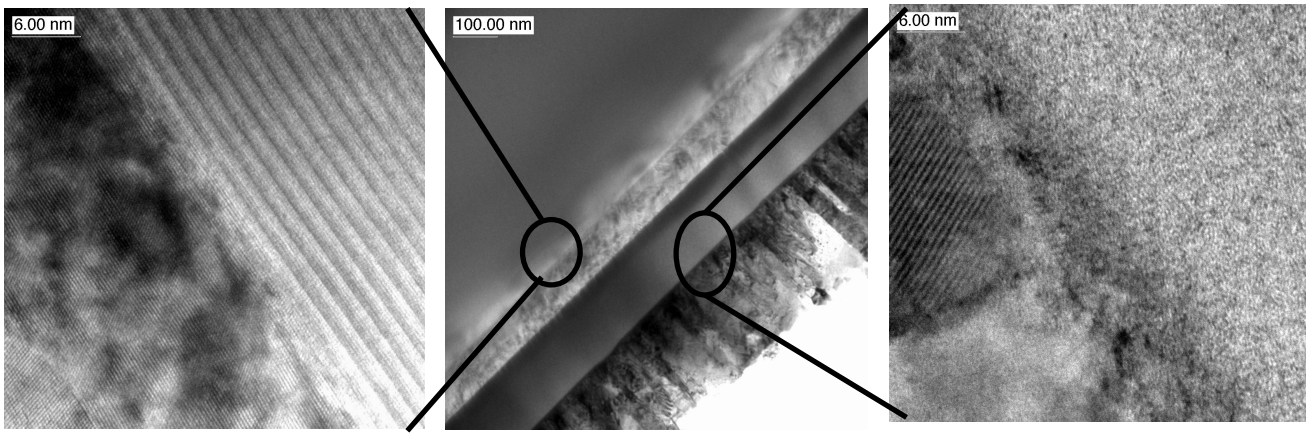

(a) (b) (c)

Figure 1: *Cross section HRTEM of a) Magnified Ti/SiC interface. b) As-deposited metallization shows the columnar multigrain structure in platinum. c) Magnified Pt/$TaSi_2$ interface.*

The SEM figure in 2a depicts the smooth Pt surface morphology after deposition. However, after 50 hours at 600°C in air, microstructural changes on the surface can be observed as shown in Fig. 2b. It reveals surface roughness in obvious contrast with Fig. 2a. This is believed to be the result of non-uniform surface oxidation of the platinum silicide, Pt_3Si [5], which is believed to

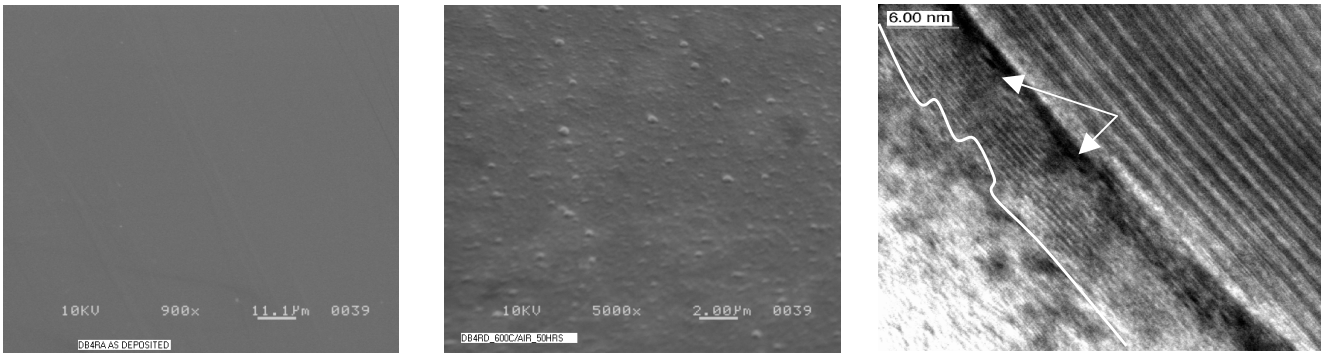

(a) (b) (c)

Figure 2. *a) SEM photomicrograph of platinum overlayer. b) Surface morphology of same sample after 600°C in air for 50 hours, revealing 2-D non-uniform oxide growth features. c) Cross-section HRTEM of SiC interface after 30-minute N_2 anneal at 600°C reveals an approximately 8nm quasi-epitaxial Ti_5Si_3 ($c \approx 0.55$ nm).*

form as a result of the decomposition of $TaSi_2$ during the initial 30-minute nitrogen anneal. Oxidation of such a non-uniform surface will therefore result in uneven volume increase as was experimentally observed in Fig. 2b. Non-uniform volume increase during surface oxidation is believed to be due to the multigrain structure of the as-deposited platinum layer as observed in the HRTEM of Fig. 1c. The HRTEM of the Ti/SiC interface after half hour nitrogen anneal at 600°C shown in Fig. 2c reveals a quasi-epitaxial layer parallel to the 6H-SiC. This layer has a periodicity of about 0.55 nm which, within limit of measurement error (7% higher), corresponds to the *c*-lattice parameter of hexagonal Ti_5Si_3 [6]. The dark feature between Ti_5Si_3 and SiC is the transition zone believed to contain stress-induced defects attributed to the lattice mismatch between Ti_5Si_3 (*a=0.743 nm*) and 6H-SiC (*a=0.308 nm*).

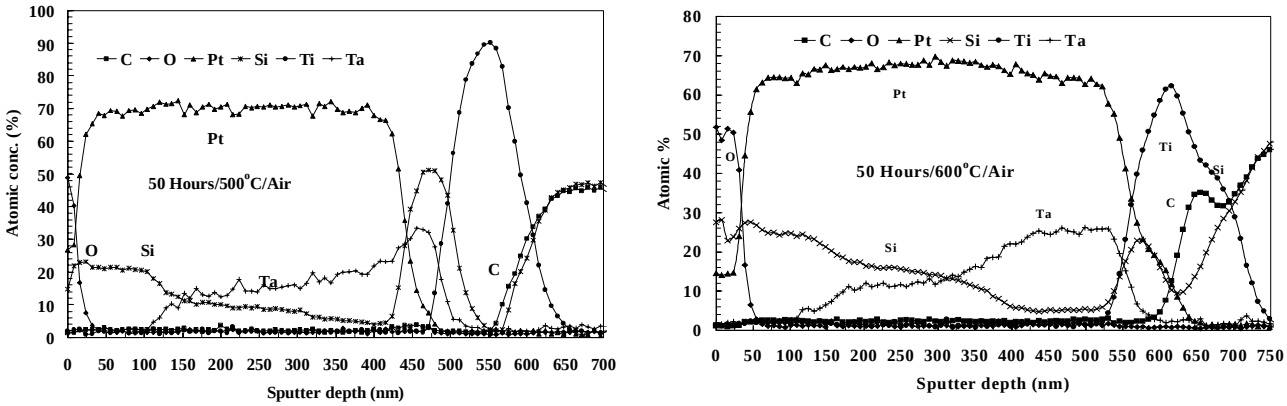

(a) (b)

Figure 3: *AES depth profiles of a) 500°C sample set treated in air for 50 hours, and b) 600°C sample set treated in air for 50 hours. Oxygen containment is observed at the surface. Ti_xC_y formation appears to have been initiated during the 600°C treatment.*

Representative AES depth profiles are shown in Figs. 3a and b for 50 hours treatment in air at 500°C and 600°C, respectively. After the 30-minute nitrogen anneal and subsequent treatment for 50 hours at 500°C (Fig. 3a), no strong evidence of TiC was observed. However, the AES depth profile shown in Fig. 3b of sample treated at 600°C in air indicated a distinct Ti_xC_y layer at about 650 nm depth, next to Ti_5Si_3.

To characterize the oxide growth kinetics, we applied the linear and parabolic rate equation expressed as [3]:

$$x^2 + Ax = B(t + \tau) \tag{1}$$

where $B = \frac{2DC_o}{C_1}$ is the parabolic rate constant (cm^2-s^{-1}); $A = 2D\left(\frac{1}{K}\right)$ is the linear rate constant (cm-s^{-1}); parabolic growth rate, D (cm^2-s^{-1}); linear growth rate, K (cm-s^{-1}); reaction time, t (s); thickness, x (cm) and $C_1=2.2\text{x}10^{22}$ cm^{-3} for SiO_2. The value of C_o is the concentration of oxygen at the surface as function of temperature and pressure. The initial thickness, x_o, and the initial time, τ, were assumed to be insignificant. The linear and parabolic growth rates of the surface oxide are respectively determined by the expressions [4]:

$$K = \frac{x_2 - x_1}{t_2 - t_1} (\text{cm-s}^{-1}) \tag{2a}$$

and $$D = \frac{x_2^2 - x_1^2}{t_2 - t_1} (\text{cm}^2\text{-s}^{-1}). \tag{2b}$$

The surface oxide was measured with both AES and HRTEM on samples heated at 500°C, 600°C, and 700°C at different time intervals. The values were substituted for x in (2a) and (2b), and together with the obtained D from equation 2b, were fitted into (1). The experimental results, together with a curve from calculation were plotted and shown in Fig. 4a for oxide growth in platinum silicide. Lie *et al* [7] and Razouk *et al* [8] confirmed that the oxidation kinetics of $TaSi_2$ have a parabolic rate constant. Our result demonstrates the parabolic oxidation characteristics of Pt_3Si.

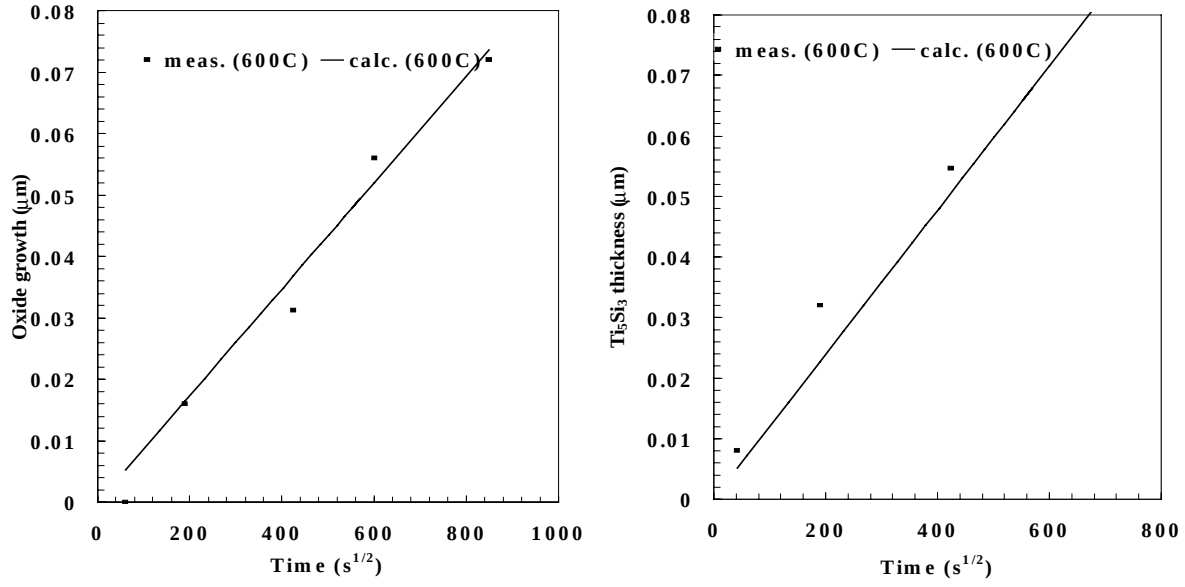

***Figure 4**: Experimental and calculated growth at 600°C in air of a) oxide in platinum silicide and b) titanium silicide.*

The growth thickness of Ti_5Si_3 is shown in Fig. 4b after 600°C for 50 hours in air. An attempt to obtain accurate growth rates beyond this time was inhibited by platinum migration toward the contact, which altered the reaction kinetics. The overall impact on the electrical and mechanical properties of the contact has not been determined. However, there is a genuine concern of a thermally driven runaway reaction if platinum appears at the interface with SiC.

Since the growth rate, *D*, is known for the temperatures between 500°C and 700°C, the activation energies for Pt_3Si oxidation and Ti_5Si_3 formation can be obtained from:

$$D = D_o \exp\left(-E_A \big/ kT\right) (\text{cm}^2\text{-s}^{-1}) \qquad (3)$$

where E_A is the activation energy (eV), *k* is the Boltzmann constant (eV-K^{-1}), and *T* is temperature (K). The parabolic growth rate obtained from equation (2b) was plotted in Arrhenius form, which then allowed for the calculation of the activation energy from the slope. Figures 5a and b show the Arrhenius plot for Pt_3Si oxidation (E_A= 1.03eV) and for Ti_5Si_3 formation from SiC (E_A= 1.96eV), respectively. The activation energy obtained for Pt_3Si oxidation is in good agreement with those obtained among a family of metal silicides that include platinum silicide [9]. The calculated activation energy for Ti_5Si_3 formation was in contrast to the value of 2.02 eV calculated from Chamberlain's work [10] for Ti_5Si_3 growth between 500°C and 700°C. A reason for the difference could be attributed to 'tailing effect' error that is typically associated with measurement by AES [11].

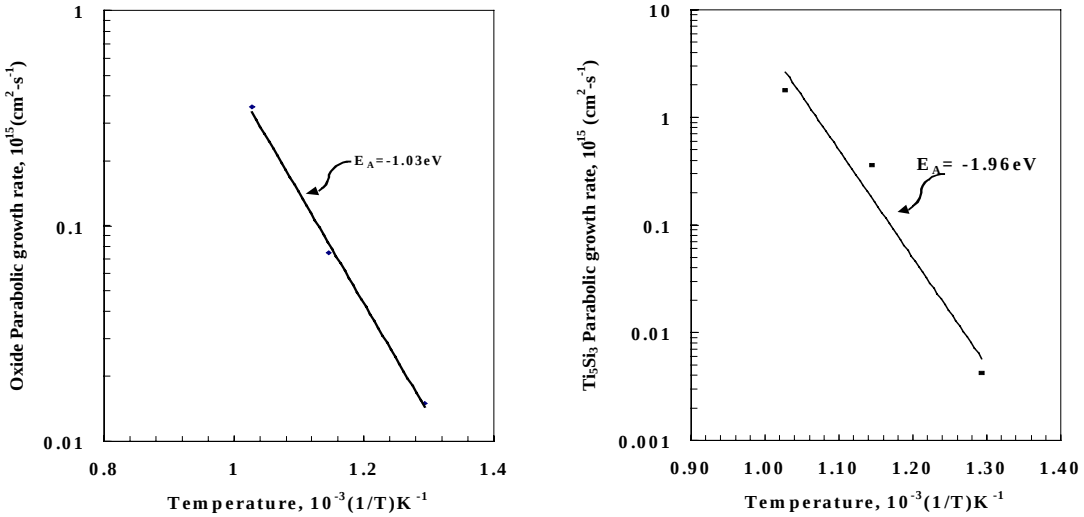

Figure 5: *Arrhenius plots of reaction rates for a) oxidation and b) Ti_5Si_3 formation at three temperature regimes, 500°C(773K), 600°C(873K), and 700°C(973K).*

To minimize this error, we used HRTEM measurements to complement the results from AES. Therefore, on the basis the more precise measurement adopted in this work, the Ti_5Si_3 growth rate obtained is likely to be more accurate.

The specific contact resistance of samples treated at 500°C and 600°C in air is shown in Figs. 6a and b, respectively. The sample treated at 500°C exhibit high values in the first 40 hours before decreasing to near constant value of about $2\text{x}10^{-4}\ \Omega\text{-cm}^2$. The sample treated at 600°C exhibited a similar trend but the duration at high values was shorter. The phenomenon is attributed to temperature and time dependent product formation at the SiC interface, which, in this case will be

accelerated at 600°C. The representative I-V characteristics after two hundred hours at 600°C, however, remained linearly ohmic, thus validating the stability of the scheme.

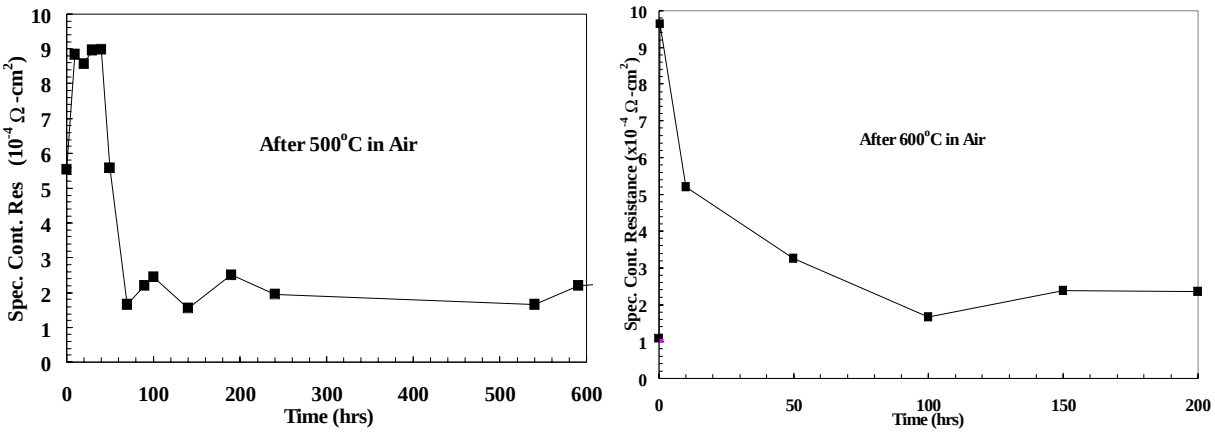

(a) (b)

Figure 6: *Specific contact resistances after intermittent heat treatment in air at a) 500°C and b) 600°C.*

CONCLUSION

Studying the reaction kinetics of two critical interfacial zones revealed fundamental insights into the thermal stability of the Ti/$TaSi_2$/Pt ohmic contact on 6H-SiC. The oxidation of the platinum silicide overlayer exhibited parabolic rate dependence, demonstrated to inhibit the migration of oxygen to the SiC interface, thereby extending the life of the contact. We also demonstrated that thermodynamically stable, quasi-epitaxial Ti_5Si_3 forms at the SiC/metal interface, providing excellent electrical contact properties. Platinum is needed for the purpose of forming a protective silicide overlayer that is also wettable for wire bonding, but its potential deleterious effect on the long-term contact stability needs to be investigated. On the basis of this result, we have thus demonstrated thermally stable specific contact resistance after a long duration exposure in air ambient at 600°C.

ACKNOWLEDGEMENT

We would like to thank Drs. Jih-Fen Lei, Gary Hunter, Larry Matus, Mary Zeller, and Phil Neudeck for their technical reviews, and Drago Androjna for the SEM images. Author RSO grateful to NASA and the Glennan Microsystems Initiative (GMI) in funding this work.

REFERENCES

1. Cree Research, Inc., Durham NC 27703 USA.
2. R. S. Okojie, D. Spry, J. Krotine, C. Salupo, and D. R. Wheeler, MRS Spring 2000, San Francisco, CA April 24-28, 2000.
3. B.E. Deal and A.S. Grove, *J. Appl. Phys.*, **36**, p. 3770-3778, (1965).
4. M. Nathan and S. W. Duncan, *Thin Solid Films*, **123** p. 69-84, (1985).
5. ASM Handbook of Alloy Phase Diagrams, Vol. 3, p. 2(347), (1992).
6. W. B. Pearson, "A Handbook of Lattice Spacings and Structures of Metals and Alloys," Vol. 2, Pergamon, London, 1967.
7. L.N. Lie, W.A. Tiller, and K.C. Saraswat, *J. Appl. Phys.*, **56**, (7), p. 2127-2132, (1984).
8. R.R. Razouk, M.E. Thomas, and S.L. Pressaco, *J. Appl. Phys.*, **53**, (7), p. 5342-5344, (1982).
9. S.P. Murarka, *Silicides for VLSI Applications*, Academic Press, New York, p. 142-143, (1983)
10. M. B. Chamberlain, *Thin Solid Films*, **72,** p. 305-311, (1980).
11. C. A. Crider, J. M. Poate, J. E. Rowe, and T. T. Sheng, *J. Appl. Phys.*, **52** (4), p. 2860-2868, (1981).